

Structural, Morphological and Optical Studies of Hydrothermally Synthesized α -Fe₂O₃@MoS₂ Composite Nanoarchitectonics

JNANRANJAN PANDA^{1†}, SUMIT MAJUMDER² and SUBHASHREE MOHNATY¹

¹Faculty of Science, Sri Sri University, Cuttack-754006, Odisha, India

²Functional Nanomaterials Group, Department of Applied Physics, School of Engineering Science, KTH Royal Institute of Technology, Hannes Alfvéns väg 12, 114 12 19 Stockholm, Sweden

†Corresponding authors email: jnanpanda@gmail.com

Present Address of the Corresponding author: Faculty of Science, Sri Sri University, Cuttack, Odisha-754006

Permanent address of the Corresponding Author: At/Po. Gud, Via-Anantapur, Dist. Balasore, Odisha-756046

Abstract: In this study, 3-dimensional dendritic structured hematite (α -Fe₂O₃) integrated with molybdenum disulfide (MoS₂) microsphere were synthesized using a facile hydrothermal approach. The structural, chemical and morphological characteristics of the as synthesized composite sample were carried out by powder x-ray diffraction (PXRD), Fourier-transform infrared (FTIR) and Field Emission Scanning Electron microscope (FESEM) respectively. The optical property of the sample was investigated by UV-Vis absorption and fluorescence emission spectroscopy. PXRD and FTIR data clearly suggests the successful synthesis of α -Fe₂O₃@MoS₂ composite. FESEM micrograph of the α -Fe₂O₃@MoS₂ composite sample demonstrate that the MoS₂ microspheres are anchored onto the dendritic arms of α -Fe₂O₃, confirming the successful synthesis of the composite sample. Fluorescence emission data of the composite sample shows the emission spectra shifts towards longer wavelength under the excitation from 340 to 400nm.

Keywords: α -Fe₂O₃@MoS₂, Hydrothermal method, Fluorescence emission.

1. INTRODUCTION:

Iron oxide-based nanostructured materials have recently garnered significant attention due to their potential applications in magnetic data storage, magnetic resonance imaging, hyperthermia, environmental

separations, gas sensing, bio-sensing, and energy storage [1-4]. Among these materials, hematite (α -Fe₂O₃) nanoparticles (NPs) stand out as the most stable iron oxide nanoparticles with semiconducting properties under ambient conditions [5, 6]. To date, various α -Fe₂O₃ structures, including one-dimensional (1D), two-dimensional (2D), and three-dimensional (3D) architectures, have been synthesized. Among these, 3D architectures of α -Fe₂O₃ often exhibit enhanced electrical, optical, magnetic, and catalytic properties compared to their 1D and 2D counterparts [5, 7]. However, the practical application of α -Fe₂O₃ is hindered by its poor electrical conductivity and high electron-hole recombination rate [6, 8]. Therefore, a specific strategy is required to enhance the optical properties of hematite based structure. One viable approach is to improve the band gap of α -Fe₂O₃ by incorporating conductive materials like molybdenum disulfide (MoS₂), which possesses a high specific surface area and excellent electrical conductivity making it an ideal candidate for improving the performance of α -Fe₂O₃-based systems.

MoS₂ has gained substantial attention due to its layered structure, similar to that of graphene, and its unique chemical, mechanical, optical and electronic properties [9, 10]. These attributes enable MoS₂ to have numerous technological applications in catalysis, optoelectronics, sensing, and energy storage [9, 10]. In recent years, several studies have reported the successful synthesis of MoS₂-based nanohybrids, such as MoS₂@RGO, MoS₂@TiO₂, MoS₂@ZnO, MoS₂@Fe₃O₄, and others. The addition of MoS₂ NPs to α -Fe₂O₃ structures not only reduces the bandgap but also enhances the specific surface area and promotes seamless integration with these oxide materials, owing to their synergistic effects. Based on the above considerations, the present research has been devoted to synthesis, characterization and study structural, morphological optical property of α -Fe₂O₃@MoS₂ composite sample. In this study, α -Fe₂O₃, MoS₂, and α -Fe₂O₃@MoS₂ composites were synthesized using a hydrothermal method. The structural, morphological, chemical and optical measurement were carried out by PXRD, FESEM, FTIR, UV-Vis absorption and fluorescence emission spectroscopy.

2. EXPERIMENTAL SECTION

2.1 Materials

Potassium ferricyanide ($K_3[Fe(CN)_6]$), sodium molybdate ($Na_2MoO_4 \cdot 2H_2O$), thiourea (CN_2H_4S), Polyvinylpyrrolidone ($(C_6H_9NO)_x$), ethanol (C_2H_5OH), were purchased from Sigma-Aldrich Co. (Bangalore, India). Deionized water (DI) was used for all experiments.

2.2 Synthesis of 3D dendritic structured α -Fe₂O₃:

Dendritic structured α -Fe₂O₃ was prepared using the hydrothermal method in the absence of MoS₂ as adopted by Majumder et. al. [5]. At first 0.264 g of $K_3[Fe(CN)_6]$ was dissolved in 80 ml DI water. The aqueous solution was then transferred into a 100 ml teflon-lined stainless steel autoclave and the hydrothermal reaction was maintained at 180 °C for 24 hours. Finally, the products were cooled to room temperature and the precipitates were centrifugally separated, cleaned with ethanol, and deionized water several times. Afterward, the collected samples were dried at 60 °C for 12 hours in an electric oven.

2.3 Synthesis of dendritic structured α -Fe₂O₃@MoS₂ composite sample:

α -Fe₂O₃@MoS₂ composite sample was developed using a facile hydrothermal synthesis route. In brief, 0.750g of sodium molybdate, 0.150g of PVP and 0.700g thiourea were dissolved in 60 ml deionized water with magnetic stirring for 30 minutes. After 30 minutes, the as-prepared 50 mg α -Fe₂O₃ was added into the solution and stirred for another 30 minutes. The solution was then transferred into a 100ml Teflon lined stainless steel autoclave and kept at 180⁰ for 24 hours. The autoclave was then allowed to cool to room temperature, and the precipitates were thoroughly washed several times with DI water and ethanol using vigorous centrifugation. Afterward, the obtained precipitates were dried at 60⁰ C for 12 hours in an electric oven. Thus α -Fe₂O₃@MoS₂ were obtained and stored for further characterization. For control experiments, pure MoS₂ were also prepared using a same technique without the introduction of α -Fe₂O₃.

2.4 Characterization Techniques:

The phase purity and crystal structure of the samples were identified by powder X-ray diffraction (PXRD) using a Bruker D8 Advanced Diffractometer using Cu K α ($\lambda = 1.54184 \text{ \AA}$) radiation operating at 35 kv and 35 mA with 2θ ranging from 10 to 80° . The surface functional groups of the synthesized samples were investigated using Fourier transform infrared spectroscopy (FTIR Magna-IR 750 Series II, Nicolet Instruments). The morphology of the sample was carried out using field emission electron microscope, FESEM (FEI, INSPECT F50). The optical measurements were acquired on a Hitachi U-3010 UV-Vis absorption spectrophotometer. The fluorescence emission spectra were performed by using an F-4500 fluorescence spectrometer with 532 nm laser excitation.

3. RESULTS AND DISCUSSION:

Initially, a 3D architecture of dendritic-structured $\alpha\text{-Fe}_2\text{O}_3$ was synthesized from $\text{K}_3[\text{Fe}(\text{CN})_6]$ using a one-step hydrothermal technique without any surface-stabilizing agent. Subsequently, PVP-mediated MoS_2 microspheres were prepared using a facile hydrothermal synthesis method, employing sodium molybdate and thiourea as the molybdenum (Mo) and sulfur (S) sources, respectively. PVP molecules were utilized to modify the surface of MoS_2 . Finally, a $\alpha\text{-Fe}_2\text{O}_3@\text{MoS}_2$ composite was developed using the same method adopted for MoS_2 synthesis. The crystallographic structure and phase purity of all the samples were confirmed through PXRD analysis. The PXRD patterns of $\alpha\text{-Fe}_2\text{O}_3$, MoS_2 , and the $\alpha\text{-Fe}_2\text{O}_3@\text{MoS}_2$ composite are shown in Fig. 1(a) and (b), respectively. The diffraction peaks of $\alpha\text{-Fe}_2\text{O}_3$ were observed at 2θ values of 24.1° , 33.5° , 35.6° , 40.8° , 49.3° , 54.2° , 57.5° , 62.5° , and 64.1° , corresponding to the (012), (104), (110), (113), (024), (116), (122), (214), and (300) planes rhombohedral hexagonal phase of $\alpha\text{-Fe}_2\text{O}_3$ [5, 6]. These values are in good agreement with the standard JCPDS card no. 33-0664. For MoS_2 , three distinct diffraction peaks were observed at 2θ values of 13.7° , 33.4° , and 58.9° , corresponding to the (002), (100), and (110) crystal planes of the hexagonal 2H- MoS_2 phase, matching the JCPDS card no. 37-1492 [11]. The PXRD pattern of the $\alpha\text{-Fe}_2\text{O}_3@\text{MoS}_2$ composite exhibited peaks at 13.9° , 24.2° , 33.1° , 35.6° , 40.8° , 49.3° , 54.2° , 62.4° , and 64.1° , indicating the coexistence of both MoS_2 and $\alpha\text{-Fe}_2\text{O}_3$ diffraction patterns. Notably,

the (104) plane of α -Fe₂O₃ overlapped with the (100) plane of MoS₂. Additionally, a decrease in the intensity of the diffraction pattern for the composite material was observed compared to the bare hematite. The obtained PXRD data shows the successful synthesis of composite material and are in good agreement with previously published literature [8].

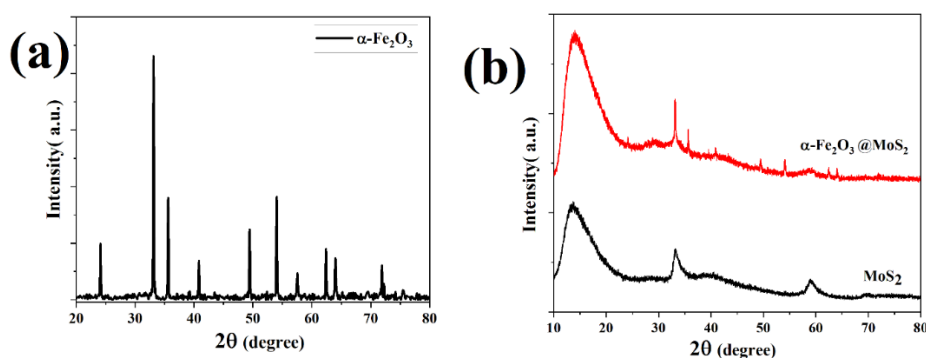


Fig. 1 (a) & (b). XRD pattern of α -Fe₂O₃, MoS₂ and α -Fe₂O₃@MoS₂

FESEM images of α -Fe₂O₃, MoS₂, and the α -Fe₂O₃@MoS₂ composite are presented in Fig. 2. The FESEM micrograph clearly illustrates the formation of 3D dendritic structures of α -Fe₂O₃. The individual α -Fe₂O₃ dendritic arms consist of a long central trunk, approximately 5–6 μ m in length, with secondary branches uniformly distributed on both sides, each measuring around 1–2 μ m in length. The FESEM micrograph of MoS₂ reveals spherical morphologies with an average diameter of 300 nm, where PVP plays a crucial role in achieving the uniform spherical morphology of the MoS₂ sample. The FESEM images of the composite material demonstrate that the MoS₂ microspheres are anchored onto the dendritic arms of α -Fe₂O₃, confirming the successful synthesis of the composite material.

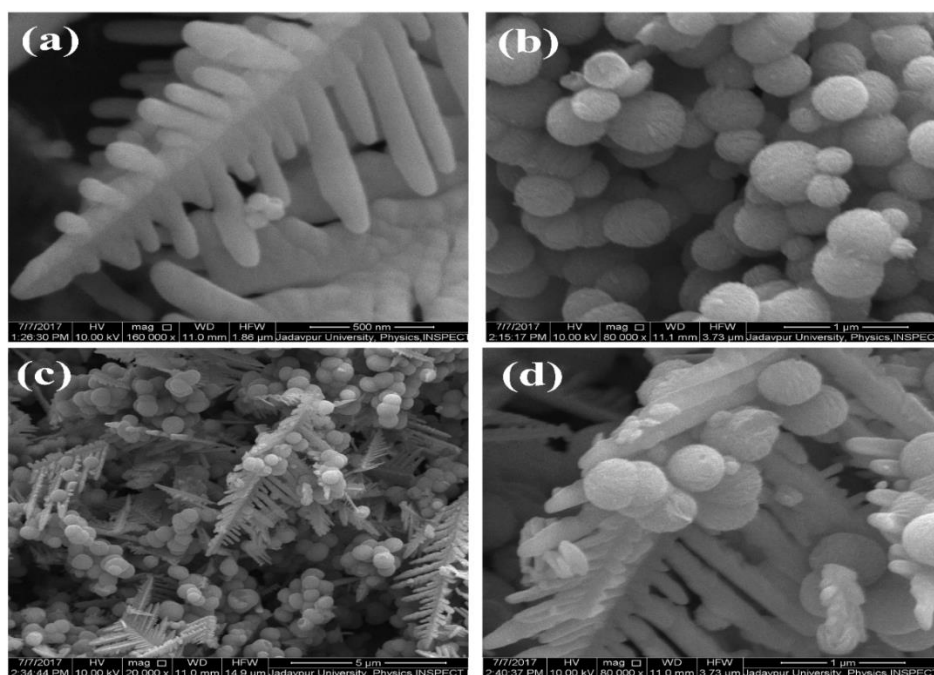


Fig.2. FESEM images of (a) α - Fe_2O_3 (b) MoS_2 (c) & (d) α - Fe_2O_3 @ MoS_2

FTIR spectrum of the all the sample is shown in Fig. 3. The transmittance peak observed at 3435 cm^{-1} and 1645 cm^{-1} show the stretching vibration of O-H bonds of the absorbed water molecules in the composite sample [9]. The peak observed at 1285 cm^{-1} corresponds to C-O stretching vibrational mode of the sample. The IR spectrum 454 and 537 cm^{-1} are attributed due to the stretching vibrational mode of the Fe-O bond confirming the presence of α - Fe_2O_3 on the composite material [5]. The peak noticed around 460 cm^{-1} corresponds to the Mo-S vibration suggesting the presence of MoS_2 in the composite material [11].

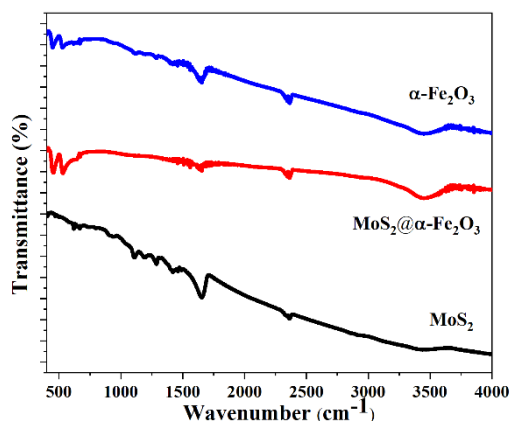


Fig. 3. FTIR spectra of α -Fe₂O₃, MoS₂ and α -Fe₂O₃@MoS₂

The optical properties of the as-synthesized samples were investigated using UV-Vis absorption and fluorescence emission spectroscopy at room temperature. In order to study, the influence of MoS₂ on the optical properties of α -Fe₂O₃, UV-Vis spectra were recorded for pure α -Fe₂O₃ and the α -Fe₂O₃@MoS₂ composite, as shown in Fig. 4(a). The absorption spectrum of pure α -Fe₂O₃ lies in the UV region; however, after integration with MoS₂ microspheres, the absorption spectrum shifts to higher wavelengths.

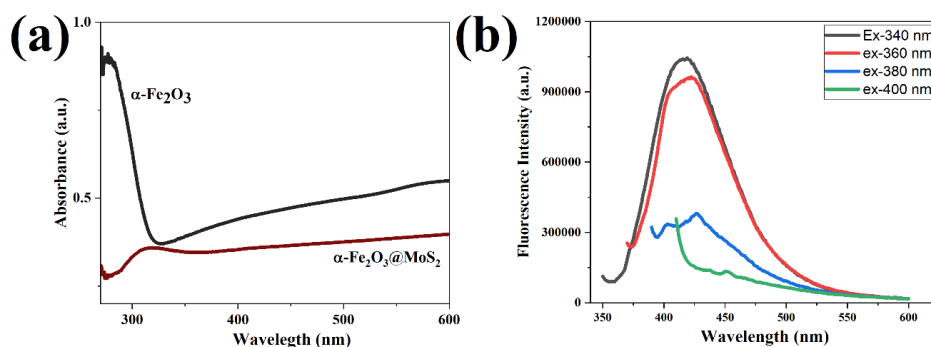


Fig. 4. (a) UV-Vis spectra of α -Fe₂O₃ and α -Fe₂O₃@MoS₂ (b) Fluorescence emission spectra of α -Fe₂O₃@MoS₂ under 340–400 nm UV-light exposure

The fluorescence emission behavior of the composite sample at various excitation wavelengths is presented in Fig. 4 (b). As the excitation wavelength increases, the emission wavelength shifts toward longer wavelengths. For instance, increasing the excitation wavelength from 340 nm to 400 nm results in a blue shift in the emission spectra, with emission wavelengths ranging from 418 nm to 445 nm. The strongest emission is noticed at 340 nm excitation. In our previous work, we observed that pure α -Fe₂O₃ exhibited an intense emission peak near 310 nm when excited at 360 nm [12]. The fluorescence intensity gradually decreases with an increase in excitation wavelength, which is consistent with the progressively reduced absorption. However, after integrating with MoS₂ microspheres, the composite sample displays an excitation dependent emission peak which may be attributed to heterogeneously distributed particles and surface states, as described in previous literature [13].

CONCLUSION:

In a nutshell, we successfully synthesized an α -Fe₂O₃@MoS₂ composite using a facile hydrothermal synthesis route. PXRD and FTIR data confirmed the successful synthesis of the α -Fe₂O₃@MoS₂ composite. Structural analysis revealed that the rhombohedral phase of α -Fe₂O₃ remained unchanged after integration with MoS₂ microspheres. FESEM results demonstrated that MoS₂ microspheres were anchored onto the dendritic arms of α -Fe₂O₃. Additionally, an excitation-dependent fluorescence emission peak was observed for the Fe₂O₃@MoS₂ composite sample.

Acknowledgments: JP is thankful to Sri Sri University, Cuttack. S.M. gratefully acknowledges Ragnar Holm Postdoctoral Scholarship, Sweden for providing a Postdoctoral research fellowship. Authors are thankful to Department of Physics, Jadavpur University, Kolkata for the instrumental facilities.

REFERENCE:

1. S. Dey, S. K. Dey, K. Bagani, S. Majumder, A. Roychowdhury, S. Banerjee, V. R. Reddy and S. Kumar, Appl. Phys. Lett. 105, 063110 (2014).
2. J. Panda, B. S. Satapathy, S. Majumder, R. Sarkar, B. Mukherjee, B. Tudu, J. Magn. Magn. Mater. 485, 165 (2019).

3. X. Zhu, J. Li, P. Peng, N. H. Nassab, and B. R. Smith, *Nano Lett.* 19 (10) 6725 (2019).
4. Y. Hu, S. Mignani, J. P. Majoral, M. Shen, X. Shi, *Chem. Soc. Rev.* 47, 1874 (2018).
5. S. Majumder, B. Saha, S. Dey, R. Mondal, S. Kumarb and S. Banerjee, *RSC Adv.* 6, 59907 (2016).
6. Q. Yin, R. Qiao, L. Zhu, Z. Li, M. Li, W. Wu, *Mater. Lett.* 135, 135 (2014).
7. S. Bharathi, D. Nataraj, M. Seetha, D. Mangalaraj, N. Ponpandian, Y. Masuda, K. Senthil and K. Yong, *Cryst. Eng. Comm.* 12, 373 (2010).
8. X. Yang, H. Sun, L. Zhang, L. Zhao, J. Lian, Q. Jiang, *Sci. Rep.*, 6, 31591 (2016).
9. P. Maiti, S. Das, J. Panda, D. Karmakar, A. Pal, S. Guha , A. Sengupta, S. Paul, P. K. Paul, *J. Phys. Chem. Sol.* 184, 111680 (2023).
10. E. Singh, P. Singh, K. S. Kim, G. Y. Yeom, and H. S. Nalwa, *ACS Appl. Mater. Interfaces*, 11 (12), 11061 (2019).
11. J. Panda and B. Tudu, *AIP Conf. Proc.* 1953, 030127 (2018)
12. S. Majumder, S. Pal, S. Kumara and S. Banerjee, *Materials Today: Proc.* 4, 5620 (2017).
13. H.H. Lin, C.X. Wang, J.P. Wu, Z.Z. Xu, Y.J. Huang, C. Zhang, *New J. Chem.* 39, 8492 (2015).